# Numerical Simulation and Parametric Study of a Single Pile in Clay Layer to Examine the Effect of Loading on Settlements and Skin Friction Distribution

Salma Al Kodsi(✉) and Kazuhiro Oda

Geotechnical Division, Department of Civil Engineering,
Graduate School of Osaka University, Osaka, Japan
salma_1987k@hotmail.com

**Abstract.** Skin friction is a shear stress distributes along pile's shaft as a reason of the movement between pile and adjacent soil. Applying loads on the pile head lead the pile to move downward and the adjacent soil to move upward resisting this movement, and a positive skin friction distribution will occur. On the other hand, applying a surcharge load on the surface next to the pile will cause extra settlements in the soil layers which may be larger than the pile settlements, and a negative skin friction (NSF) will be distributed along the pile's shaft. Load combination on both; pile and the adjacent soil, is a common reason of NSF phenomenon. To study the loading effect widely, a parametric study was carried out in this paper for different cases including pile and surcharge loading. This parametric study was held by a numerical simulation using elastic-plastic soil model defined by Matsui-Abe and the elastic-viscoplastic soil model defined by Sekiguchi-Ohta model to study the case of a single pile driven in a loaded soft clay layer. The model was first validated by comparing the results obtained from the primary consolidation with field test measurements. The comparison between two soil constitutive models was important to examine the effect of loading in different cases of soil behavior. Viscosity effect on NSF distribution was studied and shown in the graphs. As NSF may lead to pile's material fracture and structural failure, the aim of this paper is to examine the effect of loading on NSF, and clarify the viscosity behavior during primary consolidation stage. Viscous effect, surcharging and pile load combination have played a major rule in changing the skin friction distribution.

## 1 Introduction

A relative movement between pile and the soil leads to mobilize shear stresses along the interface between pile and adjacent soil. The main reason behind such movement is the application of surcharge load on the ground surface next to pile. Terzaghi and Peck (1948) assumed full mobilization of shear strength along the pile-soil interface up to the pile toe for a single pile, or along the perimeter of pile group. Therefore, the neutral point (point of zero shear stress) is assumed to be located at the bearing stratum of the

H. Khabbaz et al. (eds.), *New Prospects in Geotechnical Engineering Aspects of Civil Infrastructures*, Sustainable Civil Infrastructures,
https://doi.org/10.1007/978-3-319-95771-5_1

pile. Indraratna et al. (1992) suggested that in order to minimize NSF, piles might be driven few week, or a month after applying the surcharge load on the ground surface.

Bipul et al. (2003) presented a constitutive relationship for one-dimensional consolidation of clays. They recognized the importance of structural viscosity on clay consolidation. The viscous effect through consolidation is less at initial stage, and likely to increases gradually along with the progress of consolidation. Hanna and Sharif (2006) conducted a study on piles driven into clay and subjected to indirect loading through the surcharge applied symmetrically on the surrounding area. The study was based on a numerical model using a finite element technique and the soil was assumed to follow a linear elastic-perfectly plastic stress-strain relationship, which defined by Mohr-Coulomb failure criterion. They concluded that negative friction is developed on the pile's shaft during the undrained period and continues to exist until the consolidation of the surrounding soil be fully completed under surcharge loads. Tung-Lin (2009) studied the effect of viscosity on consolidation of poroelastic soil due to groundwater table depression. He showed that the displacement and pore water pressure of clay stratum are strongly related to the viscosity effect. The overestimation of soil displacement will occur only when the viscosity effect is being neglected. Werjuan et al. (2012) studied NSF of the super long pile caused by soil settlement under large-scale surcharge loading. They showed the impact of NSF and to what extent the soil parameters surrounding pile affect the NSF distribution. In their series of model tests on NSF on single pile and pile groups under different surcharge loading conditions, Ting et al. (2016) found that pile head settlement and NSF under side load were smaller compared with the result of the test under uniform loading, while the location of neutral plane (LNP) was lower. Arpan and Sujit (2017) developed a 3-D consolidation apparatus and performed a series of 3-D consolidation test under different surcharge pressures. They concluded that the consolidation characteristics were largely affected by the surcharge pressure. Increasing the surcharge on the surrounding soil makes it denser to reduce both the lateral movements of soil particles, and the lateral pore water pressure.

Many researchers studied the effect of surcharging on the NSF distribution, however the objective of this paper is to study the effect of the combination of surcharging and pile load on the distribution of shear stresses along the pile length besides the effect of viscosity during primary consolidation compared to elastic-plastic behavior. An elastic-viscoplastic and elastic-plastic soil models were represented herein to carry on the parametric study. A field test of a single pile was used to validate the model and conduct the numerical study.

## 2 Methodology

### 2.1 Field Loading Test

Matsui (1993) carried out a full-scale loading test of a cast-in-place RC bored pile in Osaka bay, Osaka, Japan. The soil profile consisted of both Holocene Deposits and Upper Pleistocene Deposits. The Holocene layers consisted of loose and soft silts and clays. A sandy gravel layer was adopted as a bearing layer of the tested pile. The tested pile was a cast-in-place RC pile with 1.5 m in diameter and 28.5 m in length. The vertical loading test was carried out, in accordance with the Standard of the JGS (JGS 1972). Figure 1 shows the field test soil section.

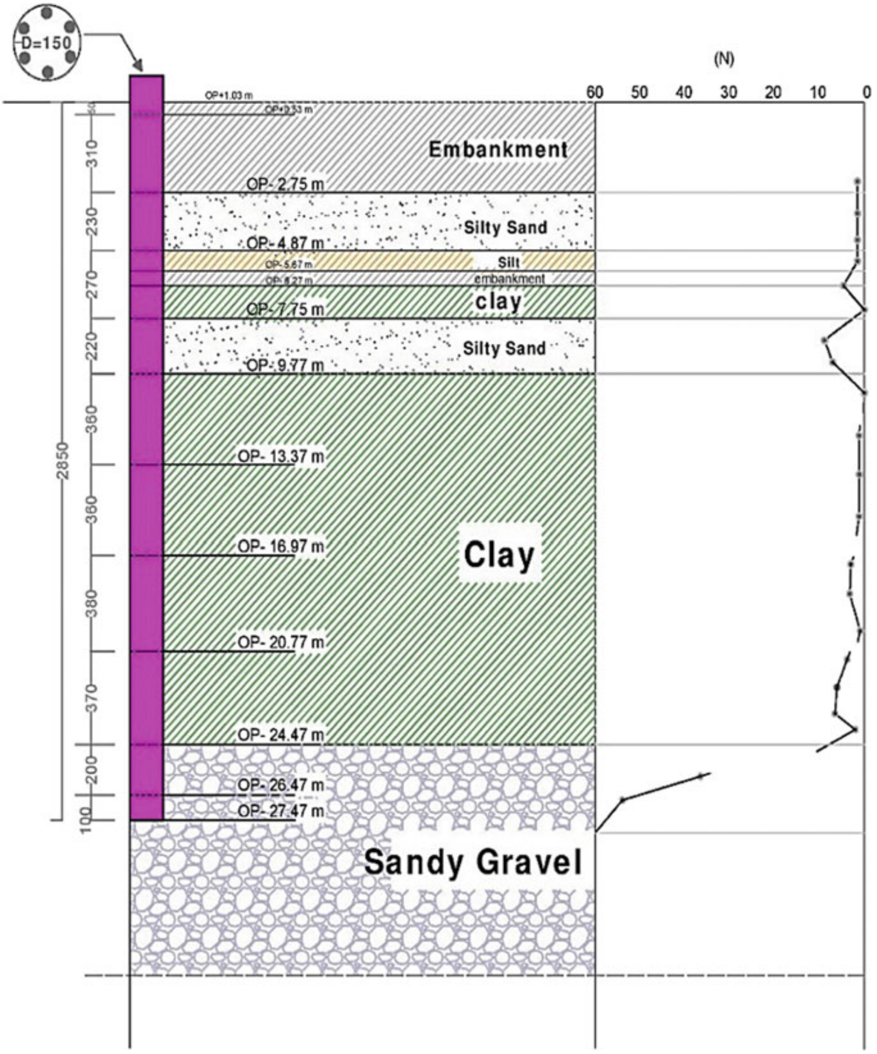

**Fig. 1.** Field test section

## 2.2 Numerical Model

### 2.2.1 Soil Constitutive Models

Finite element analysis was performed in order to compare results obtained from field test measurements with those from the numerical model. The model is an axisymmetric model assumes to behave as elastic-plastic material to represent the correlation between the stresses and the strains due to Matsui and Abe (1981) constitutive soil model for the main clay layer. This elastic-plastic soil model will be compared with the elastic-viscoplastic soil constitutive model represented by Sekiguchi and Ohta (1977). The different between these two soil models is the time dependency. Although elastic-plastic soil model is a time-dependent stress strain model but the viscous effect has been noticed during primary consolidation which affected the soil settlements. Elastic-plastic model is represented by Matsui-Abe in Eqs. (1) and (2). The Sekiguchi-Ohta model is a Cam-Clay type effective stress model for the behavior of clay-type soils and the yield surface (f) is given by Eq. (3). The bearing layer behavior was represented by Yasufuku model in Eq. (4).

$$e_0 - e = \lambda \ln\left(\frac{p'}{p'_0}\right) + (\lambda - \kappa)\left(\frac{\alpha_a}{\alpha_a - 1}\right)\ln\left\{\frac{M_a + (\alpha_a - 1)\eta}{M_a + (\alpha_p - 1)\eta_{k0}}\right\} \tag{1}$$

For the active state

$$e_0 - e = \lambda \ln\left(\frac{p'}{p'_0}\right) + (\lambda - \kappa)\left(\frac{\alpha_p}{1 - \alpha_p}\right)\ln\left\{\frac{M_p + (1 - \alpha_p)\eta_{k0}}{M_p + (1 - \alpha_p)\eta}\right\} \tag{2}$$

For the passive state

where e is the void ratio, $e_0$ is the initial value of e, λ is the compression index, κ is the swelling index and $\alpha_a$, $\alpha_p$ are the strain increment ratio.

$$f = \mu \ln\left|\frac{1}{\delta}\left[\left\{1 - \exp\left(-\frac{\delta \dot{v}_r^v}{\mu}t\right)\right\}\exp\left(\frac{v^p}{\mu}\right) + \delta \exp\left(-\frac{\delta \dot{v}_r^v}{\mu}t\right)\right]\right| - v^{vp} = 0 \tag{3}$$

where μ is the coefficient of secondary consolidation, $\dot{v}_r^v$ is the reference viscous volume strain rate, δ is a material constant and $v^p$ is the plastic volumetric strain.

$$f = \ln\frac{p}{p_0} + \frac{C}{2(C-1)}\ln\left[\frac{(1-C)(2\alpha - \eta)\eta + \{N - (2-C)\alpha\}N}{(1-C)\alpha^2 + \{N - (2-C)\alpha\}N}\right] = 0 \tag{4}$$

model in Eq. (4)

Where N and C are experimental parameters, α is an internal parameter to reflect the influence of the proportional loading path on the yield surface and $\eta = \frac{q}{p'}$ is the stress ratio.

### 2.2.2 Model Boundary, Mesh and Initial Conditions

The surface of the top layer is assumed to be permeable while the low and side boundaries of the model are supposed to be impermeable. The level of the ground water is at 0.80 m down from the surface. The low model boundary is being fixed, while the boundaries at the axis of symmetry and sides are free to move vertically.

The mesh was divided into 13 blocks. The first block -the pile- is divided into 360 elements behave as elastic material. The main clay layer includes block (2) and block (3) which both are divided into 234 elements. The abruption between pile shaft and

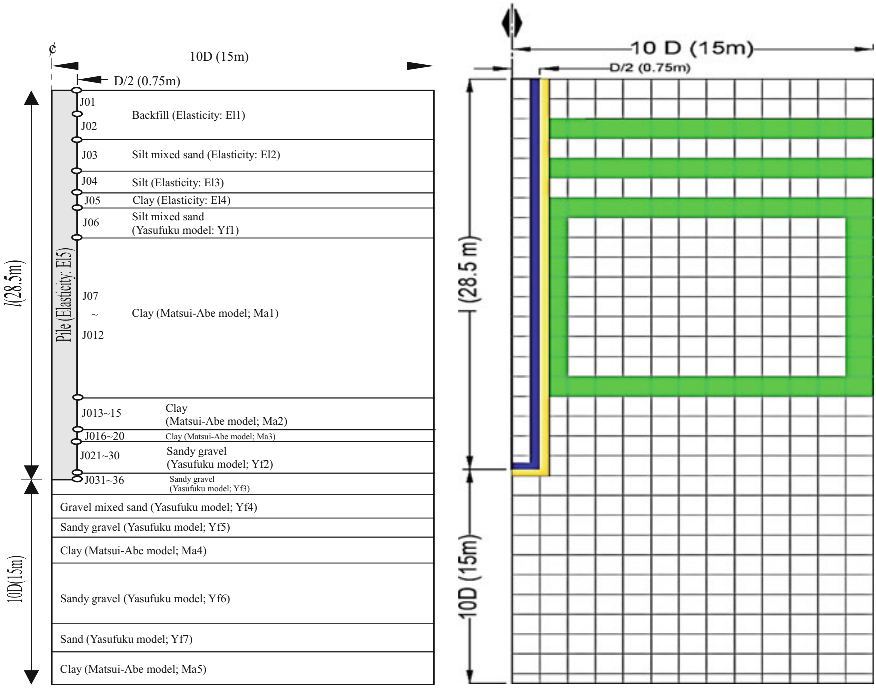

**Fig. 2.** Numerical model and the mesh

surrounding soil is represented by 36 joint elements (Goodman et al. 1968) in which the main clay layer includes 6 joint elements. Figure 2 shows the analytical study model and mesh boundary.

## 2.3 Model Validating

Numerical modelling using the finite elements technique was used herein to validate the used model. Table 1 shows the analytical elastic parameters for the pile material. Table 2 describes the basic mechanical constants for clay in Elastic-plastic behavior by Matsui-Abe. The main parameters for Sekiguchi-Ohta model are mentioned in Table 3 Yasufuku basic parameters for the bearing soil layer are shown in Table 4. Finally, the parameters of joint elements for the main clay layer are shown in Table 5. All parameters were determined through soil investigations including SPT and CPT (after Oda 2012).

A comparison between the measured axial forces and predicted values by the present numerical model is shown in Fig. 3. It can be noticed from the comparison results that the numerical model is valid to carry on the parametric study.

**Table 1.** Analytical parameters of elasticity

| No. | E (kN/m$^2$) | υ |
|---|---|---|
| E11 | 8.40E+04 | 0.47 |
| E12 | 2.70E+04 | 0.47 |
| E13 | 3.00E+04 | 0.35 |
| E14 | 1.50E+04 | 0.30 |
| E15 | 2.20E+07 | 0.22 |

**Table 2.** Analytical parameters of Matsui-Abe model

| No. | λ | κ | M |
|---|---|---|---|
| Ma1 | 0.2480 | 0.0124 | 1.41 |
| Ma2 | 0.4950 | 0.0248 | 1.26 |
| Ma3 | 0.4000 | 0.0248 | 1.26 |
| Ma4 | 0.5800 | 0.0243 | 1.26 |
| Ma5 | 0.4480 | 0.0224 | 1.32 |

*Note* λ is the slope of normally consolidation line, κ is the slope of elastic swelling line and M is the frictional constant. Poisson ratio (υ) = 0.333

**Table 3.** Analytical parameters of Sekiguchi-Ohta model

| No. | λ | κ | M |
|---|---|---|---|
| Se1 | 0.1024 | 0.01240 | 1.47 |
| Se2 | 0.2475 | 0.01240 | 1.41 |
| Se3 | 0.2475 | 0.01240 | 1.41 |
| Se4 | 0.4950 | 0.02480 | 1.41 |
| Se5 | 0.5800 | 0.02430 | 1.26 |

*Note* $\mu = 0.002, \delta = 1.0 \times 10^{-10}$ *and* $v_0 = 1.0 \times 10^{-10} (1/\mathrm{min})$

**Table 4.** Analytical parameters of Yasufuku model

| No. | N | M |
|---|---|---|
| Yf1 | 1.90E−02 | 0.75 |
| Yf2 | 2.82E−03 | 0.80 |
| Yf3 | 2.82E−03 | 0.75 |
| Yf4 | 2.82E−03 | 0.75 |
| Yf5 | 3.27E−03 | 0.80 |
| Yf6 | 2.82E−03 | 0.8 |
| Yf7 | 3.27E−03 | 0.75 |

*Note* α, Cg and Cf are constants. α = 0.4, Cg = 2.0, Cf = 1.5

**Table 5.** Analytical parameters of joint elements

| No. | Kn (kN/m$^3$) | Ks (kN/m$^3$) | C0 (kN/m$^2$) |
|---|---|---|---|
| J07 | 9.8E+09 | 9.8E+09 | 5.64 |
| J08 | 9.8E+09 | 9.8E+09 | 17.29 |
| J09 | 9.8E+09 | 9.8E+09 | 15.90 |
| J10 | 9.8E+09 | 9.8E+09 | 11.52 |
| J11 | 9.8E+09 | 9.8E+09 | 15.01 |
| J12 | 9.8E+09 | 9.8E+09 | 10.97 |

*Note* Kn, Ks are the slope of elastic line in compression state and shear deformation state, respectively, C0 is cohesion factor between pile shaft and surrounding soil. $\theta$ is the internal angle of friction = 0

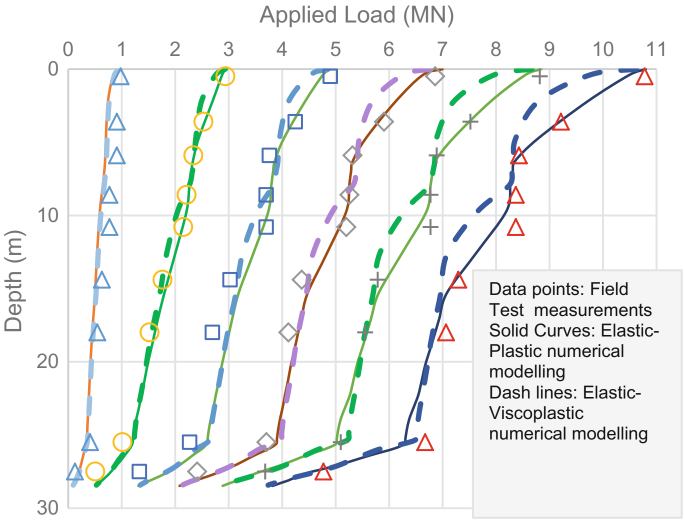

**Fig. 3.** Pile axial load distribution

## 3 Parametric Study

The aim of this parametric study is to examine different types of loading, to observe the behavior of both soil and pile, and to study the loading cases effect on settlements and skin friction distribution. The study is based on two types of loading;

① S: First, applying the pile load and then applying the surcharge load on the ground surface next to pile head (i.e. no surcharging on pile).

② P + S: First, applying the pile load and then applying the surcharge load on both ground surface and pile head (i.e. all model surface is under surcharging).

**Table 6.** Loading cases for the parametric study

| Case | PL$^a$ | SL$^b$ | S | P + S | Case | PL$^a$ | SL$^b$ | S | P + S |
|---|---|---|---|---|---|---|---|---|---|
| 1 | 100 | 2.0 | ✓ | | 5 | 100 | 8.0 | ✓ | |
| 2 | 100 | 2.0 | | ✓ | 6 | 500 | 2.0 | | ✓ |
| 3 | 100 | 4.0 | | ✓ | 7 | 1100 | 2.0 | | ✓ |
| 4 | 100 | 6.0 | ✓ | | | | | | |

$^a$Pile load (tf), $^b$Surcharge load (tf/m$^2$)

In the light of these two types of loading, Table 6. was found to clarify the parametric study of loading cases.

The following figures present the effect of loading and viscosity on the settlements, axial force and skin friction distribution. Figure 4 shows the pile axial load distribution for elastic-viscoplastic model. When applying a small value of surcharging, larger distribution was examined along pile's shaft in regarding to comparing viscosity with elastic-plastic. In the contrary, in the light of large surcharging, the difference in the distribution in two models did not occurred. A comparison of the case of small and large surcharging in two soil models is shown in Fig. 5.

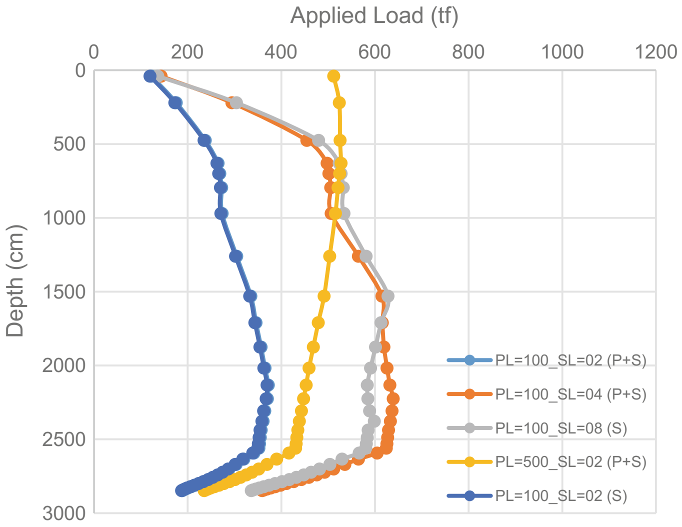

**Fig. 4.** Pile axial load distribution/elastic-viscoplastic model

The ground settlements with time for the two soil models and different cases of loading are shown in Figs. 6 and 7. Viscous effect had a major influence on soil settlements, where this influence played a rule in case of applying a small surcharging while bigger surcharge load leaded to a small different in the settlements values between elastic-plastic and elastic-viscoplastic soil models and that is clarified in

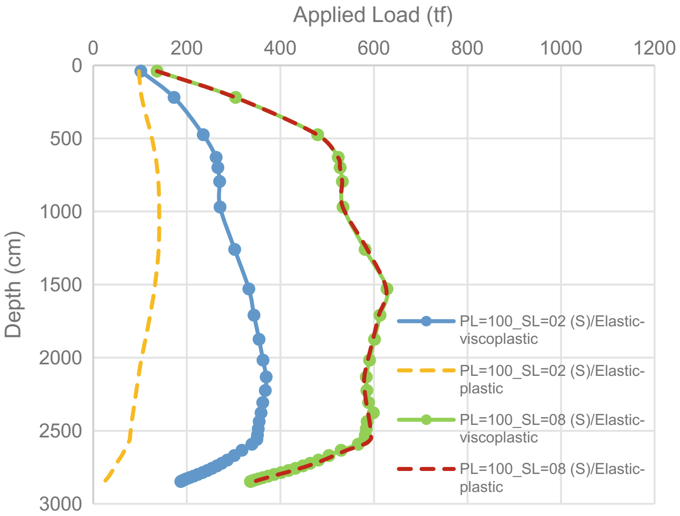

**Fig. 5.** Pile axial load distribution/comparison between elastic-plastic and elastic-viscoplastic model

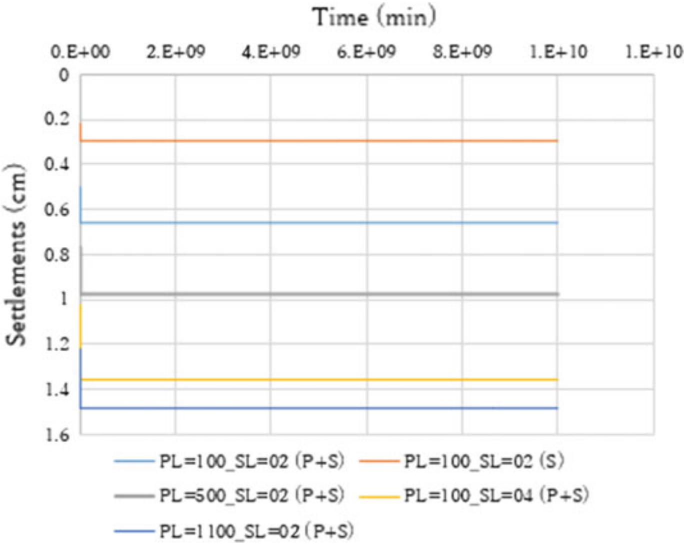

**Fig. 6.** Ground settlements with time/elastic-plastic model

Fig. 8. Changing the applied pile load to a specific value occurred the pile to settle more than the ground, whereas this conclusion can be shown in Figs. 9 and 10 for two cases of pile loading.

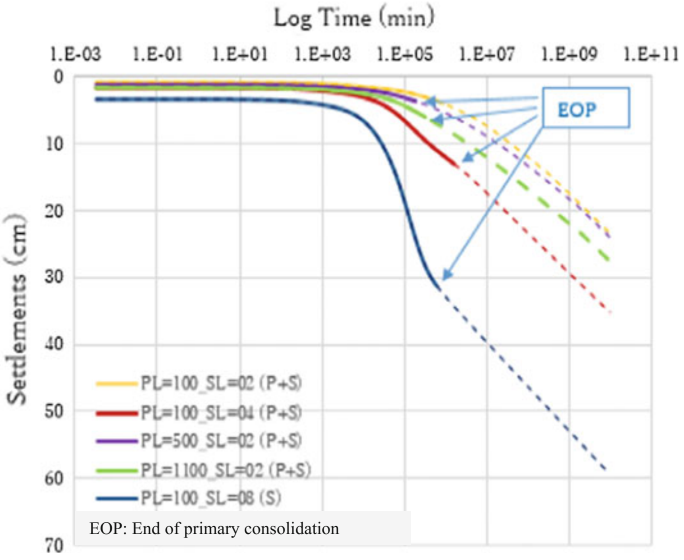

EOP: End of primary consolidation

**Fig. 7.** Ground settlements with time/elastic-viscoplastic model

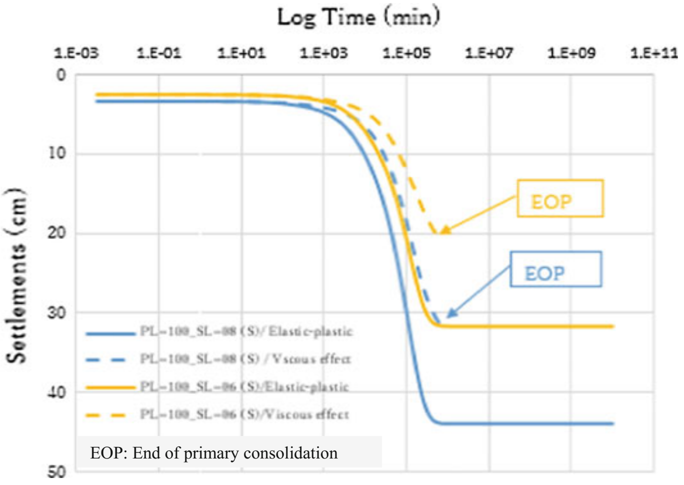

EOP: End of primary consolidation

**Fig. 8.** Ground settlements with time/comparison between elastic-plastic and elastic-viscoplastic model

As the distribution of skin friction is related to pile and soil settlements, same conclusion was observed in Figs. 11 and 12, whereas applying a small surcharge load leaded to a bigger skin friction distribution in case of viscosity. Figure 13 shows the case of applying a larger pile load which changed the distribution of NSF into a positive skin friction.

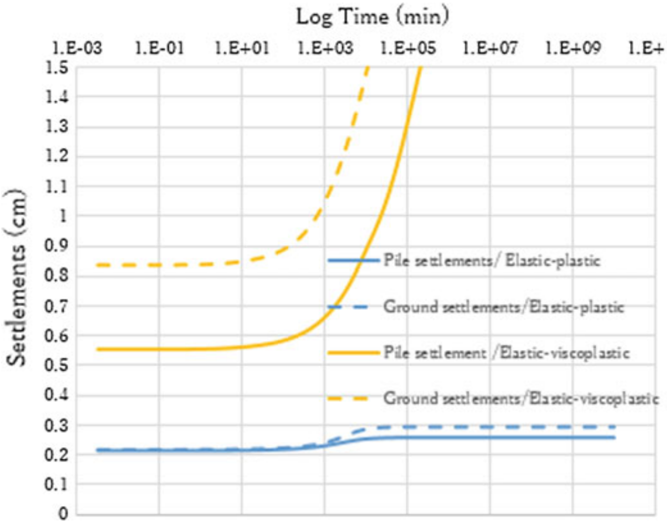

**Fig. 9.** Ground and pile settlements with time/PL = 100_SL = 02 (S)

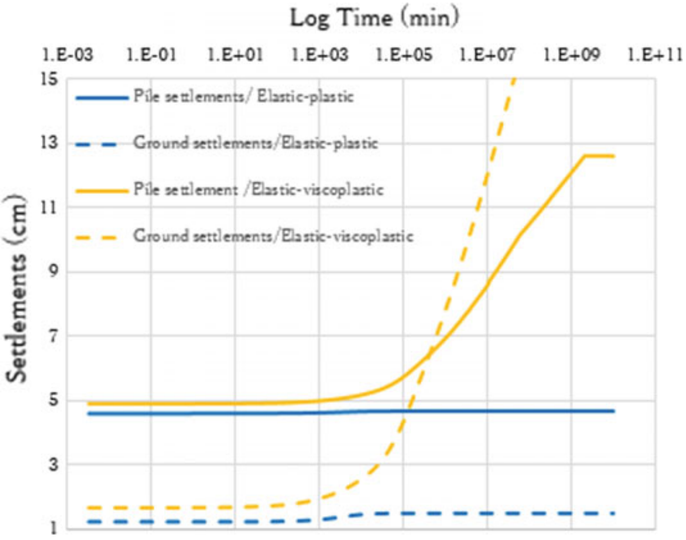

**Fig. 10.** Ground and pile settlements with time/PL = 1100_SL = 02 (P + S)

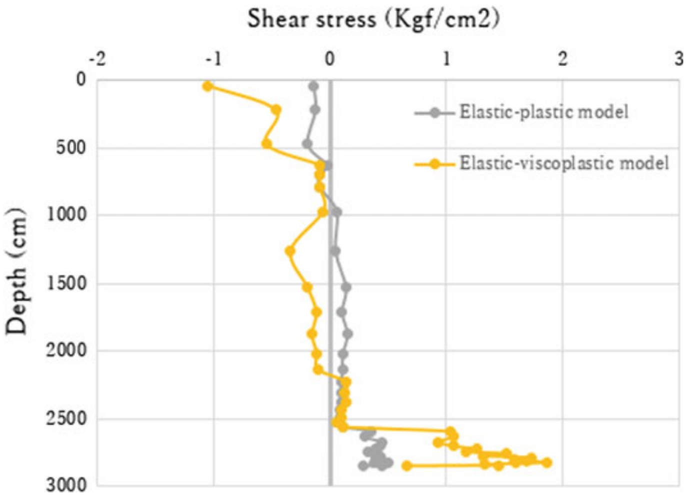

**Fig. 11.** Shear stress distribution/comparison between elastic-plastic and elastic-viscoplastic model (PL = 100_SL = 02(S))

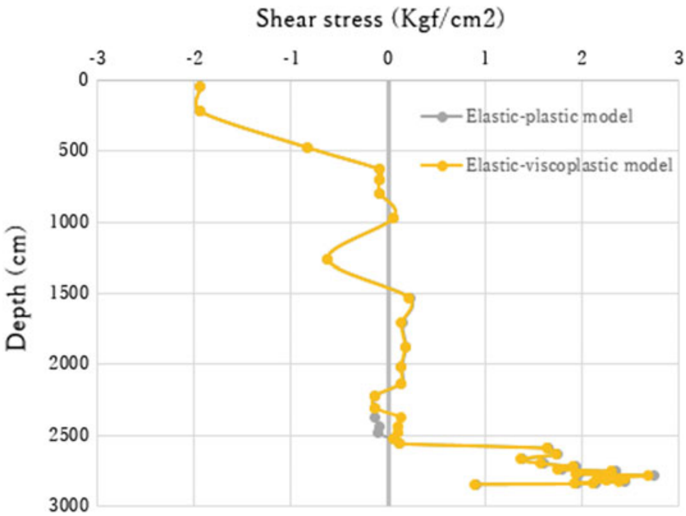

**Fig. 12.** Shear stress distribution/comparison between elastic-plastic and elastic-viscoplastic model (PL = 100_SL = 08 (S))

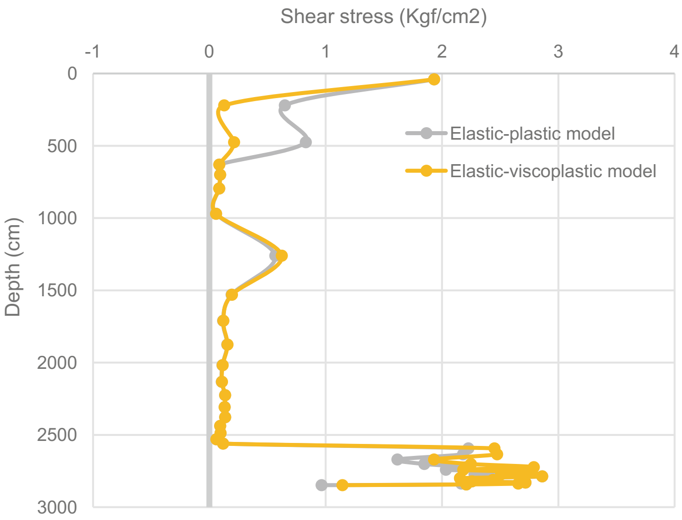

**Fig. 13.** Shear stress distribution/comparison between elastic-plastic and elastic-viscoplastic model (PL = 1100_SL = 02(P + S))

## 4 Conclusions

Surcharging and pile load play a vital role in mobilizing shear stresses along the pile's shaft (negative and positive friction) regardless the used soil model in analysis. In this paper two different soil models were used and a parametric study for different loading cases was mentioned. It can be concluded that:

- Surcharging is the main reason of soil settlements and NSF mobilizing and its effect will be more significant when it's applied only on the ground surface next to the pile.
- When the whole model surface is under surcharging and the pile head is loaded, the NSF will be smaller comparing with the case of surcharging is applied on the ground surface only. Adding an extra load to the pile, leads the pile at specific point to settle equal or more than the adjacent soil which reduces NSF.
- Viscous effect has a major role in increasing the soil settlements and skin friction distribution even though the study has been done during the primary consolidation stage. This effect will be noticed clearly in case of small values of surcharging but when the surcharge load exceeded a specific amount, the viscous influence was approximately similar to elastic-plastic.
- It is important to take the viscous effect into consideration when designing pile foundations. Carrying on this study to examine the soil behavior and skin friction distribution during secondary consolidation due to structural viscosity is also important and must be covered through future researches.

## References

Arpan, L., Sujit, K.P.: The effect of different surcharge pressure on 3-D consolidation of soil. Int. J. Appl. Eng. Res. **12**(8), 1610–1615 (2017). ISSN 0973-4562

Awwad, T., Kodsi, S.A.: A comparison of numerical simulation models to determine the location of neutral plane. In: Proceedings of the 19th International Conference on Soil Mechanics and Geotechnical Engineering, pp. 1947–1950 (2017)

Awwad, T., Donia, M., Awwad, L.: Effect of a stiff thin Foundation soil layer's depth on dynamic response of an embankment dam. Proc. Eng. **189**, 525–532 (2017)

Bipul, C.H., Balasingam, M., Goro, I.: Viscosity effects on one-dimensional consolidation of clay. Int. J. Geomech. **3**(1) (2003)

Hanna, A., Sharif, A.: Negative skin friction on single piles in clay subjected to direct and indirect loading. Int. J. Geomech. (2006)

Indraratna, B., Balasubramaniam, A. S., Phamvan, P., Wong, Y.K.: Development of negative skin friction on driven piles in soft Bangkok clay. Can. Geotech. J. **29**, 393–404 (1992)

Matsui, T.: Case studies on cast-in-place bored piles and some considerations for design. Deep Foundations on Bored and Auger Piles. Ghent, pp. 77–101 (1993)

Matsui, T., Abe, N.: Multi-dimensional elasto-plastic consolidation analysis by finite element method. Soils Found. **21**(1), 79–95 (1981)

Oda, K.: Numerical simulations of field loading tests of cast-in-place bored piles with large diameter. In: International Conference(Proceedings) on Testing and Design Methods for Deep Foundations, pp. 859–866 (2012)

Poorooshasb, H.B., Alamgir, M., Miura, N.: Negative skin friction on rigid and deformable piles. Comput. Geotech. **18**(2), 109–126 (1996)

Sekiguchi, H., Ohta, H.: Induced anisotropy and time dependency in clays. In: 9th ICSMFE, Tokyo, Constitutive Equations of Soils, pp. 229–238 (1977)

Terzaghi, K., Peck, R.B.: Mechanics in Engineering Practice. Wiley, New York (1948)

Ting, H., Liangde, H., Lijun, H.: The influence of surcharge load on the negative skin friction on pile groups. In: Proceedings of Twenty-Sixth (2016) International Ocean and Polar Engineering Conference, Rhodes, Greece, 26 June–1 July 2016

Tung-Lin, T.: Viscosity effect on consolidation of poroelastic soil due to groundwater table depression. Environ. Geol. **57**, 1055–1064 (2009)

Werjuan, Y., Yimin, L., Jun, C.: Characteristics of negative skin friction for super long piles under surcharge loading. Int. J. Geomech. **12**(2) (2012)